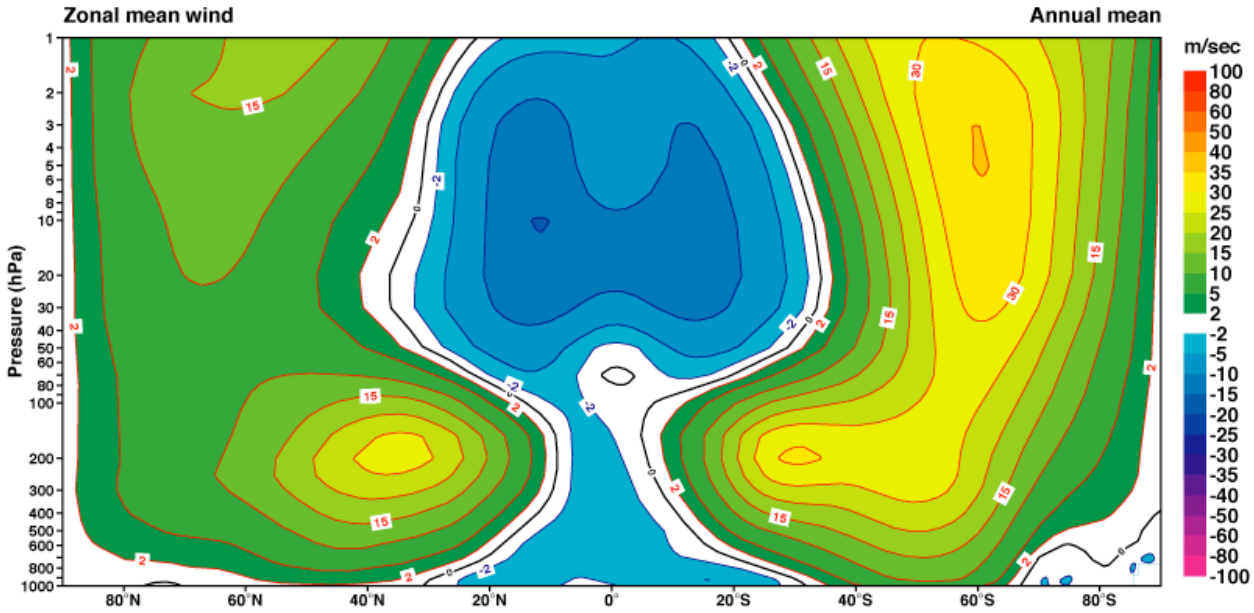

Figure 2.1 Pole-to-pole cross-section of the climatological mean annual mean [*u*] based upon the ERA-40 Reanalysis from 1979 through 2001. Pressure is plotted on a logarithmic scale so that distance above the baseline is nearly proportional to geometric height. It should be kept in mind that the density drops off by about three orders of magnitude from the bottom to the top of these sections. Hence, the mass-weighted angular momentum is dominated by the features at the lower levels.

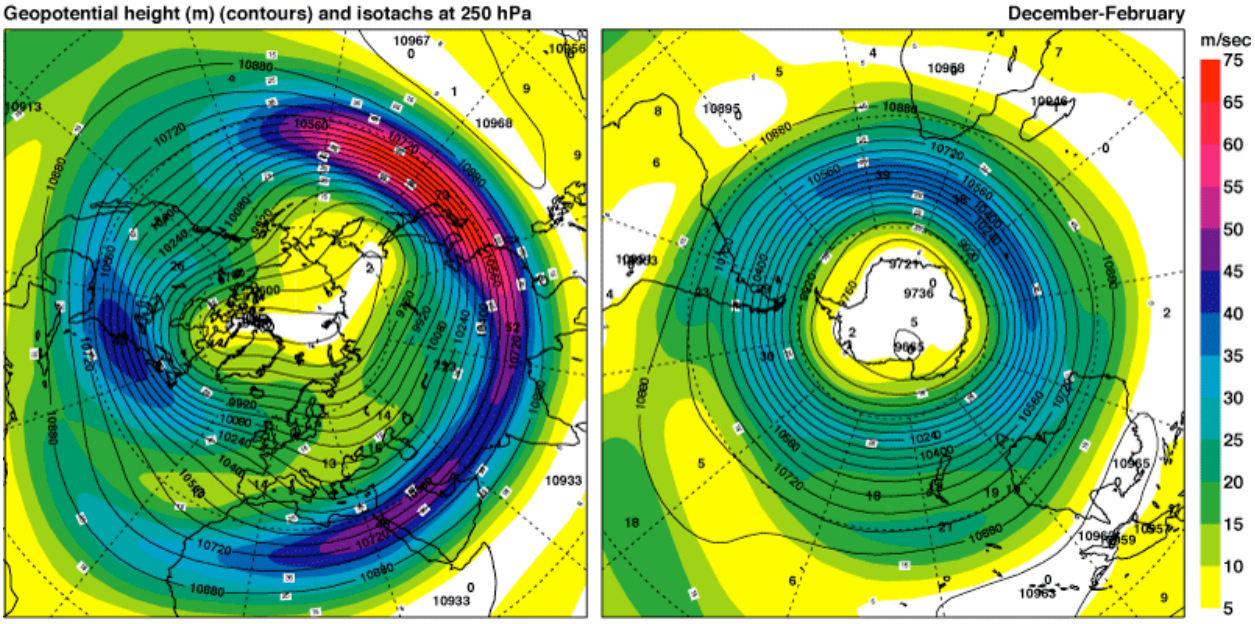

Fig. 2.2 Climatological mean wind speed at the 250 hPa level: DJF (upper panels) and JJA (lower panels). In the regions of strong winds it is virtually identical to the distribution of zonal wind *u* , since jetstreams tend to be zonally oriented.

Diagrams for Chapter 2

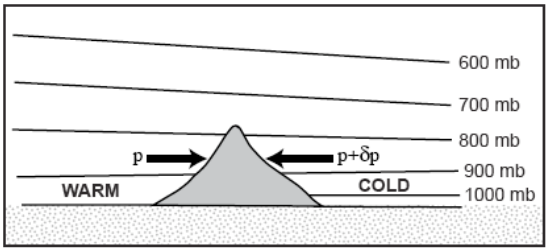

Fig. 2.3 Pressure force exerted on the atmosphere by an idealized mountain range.

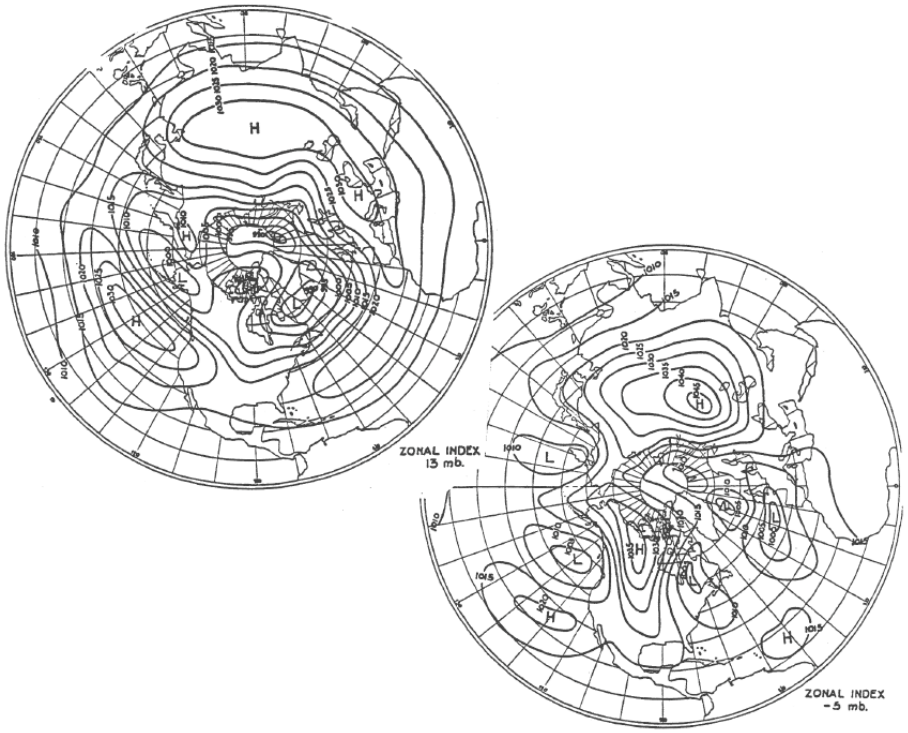

Fig. 2.4 Composite sea-level pressure patterns for "high and low index" circulation regimes, based upon the zonally averaged sea-level pressure gradient between 35 and 55°N. After Willett (1944).

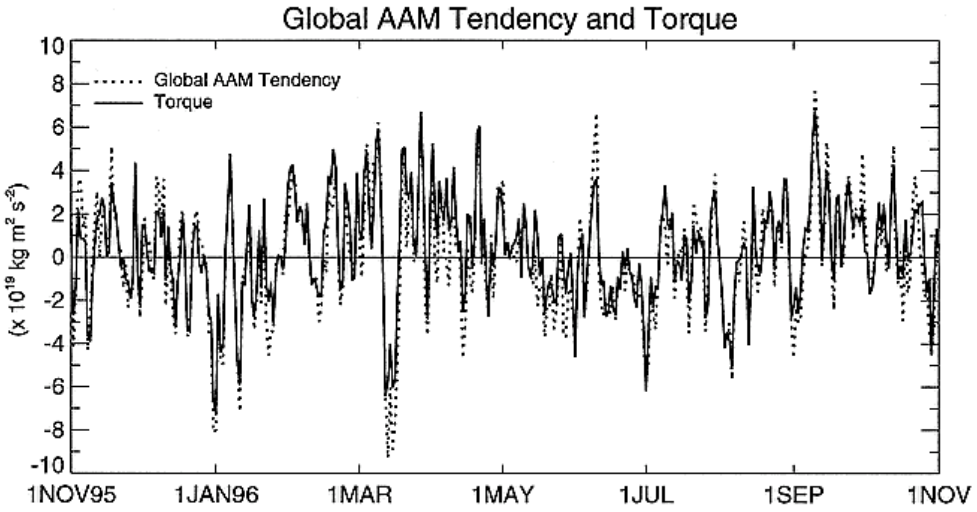

Fig. 2.5 Daily time series of the global AAM tendency (dotted) and the sum of the global friction and mountain torque (solid) for the period 1 November 1995–1 November 1996. Units are 10^{19} kg m^2 s^{-2}. After Iskenderian and Salstein (1997)

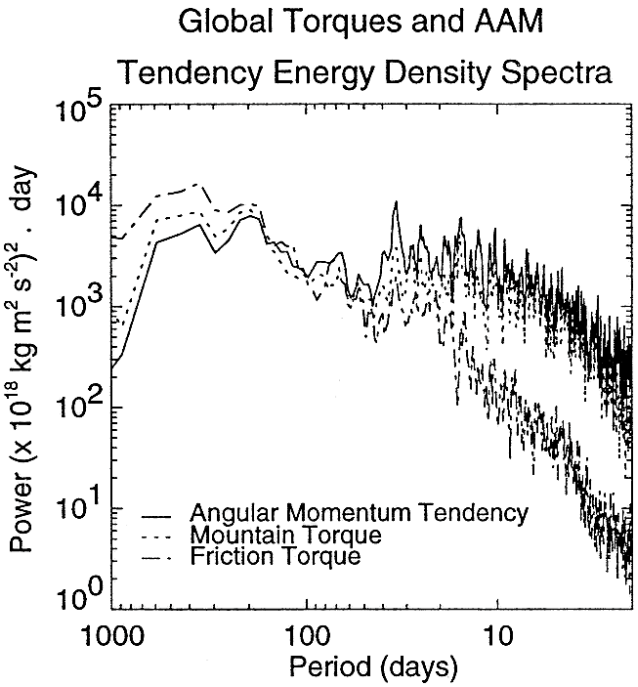

Fig. 2.6 Log–log power spectrum with period of global angular momentum tendency (solid), global mountain torque (dotted), and global friction torque (dash–dot) based upon data for the period February 1992 to November 1996. Units are $(10^{18}$ kg m^2 $s^{-2})^2$ day. The periodogram is smoothed using a five-point moving average in frequency. After Iskenderian and Salstein (1997).

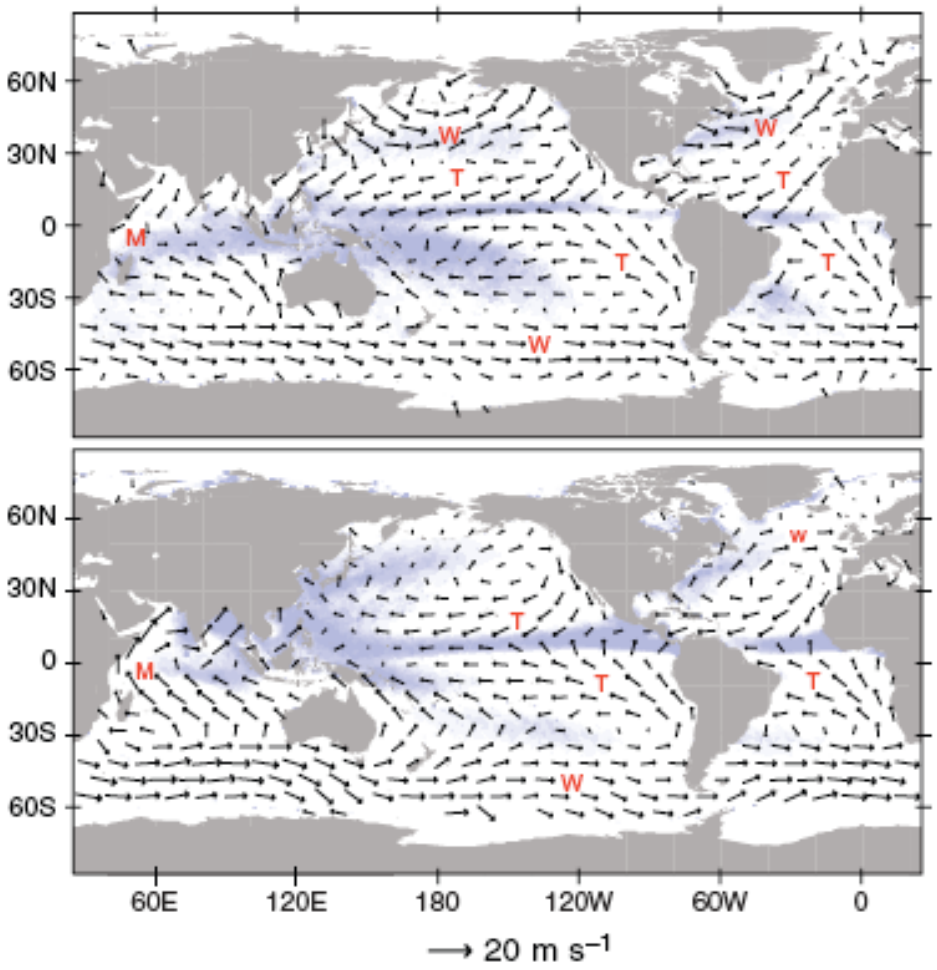

Fig. 2.7 December–January–February (top) and June–July–August (bottom) surface winds over the oceans based on 3 years of satellite observations of capillary waves on the ocean surface. The bands of lighter shading correspond to the major rain belts. **M**'s denote monsoon circulations, **W**'s westerly wind belts, and **T**'s trade winds. The wind scale is at the bottom of the figure. [Based on QuikSCAT data. Courtesy of Todd P. Mitchell.]

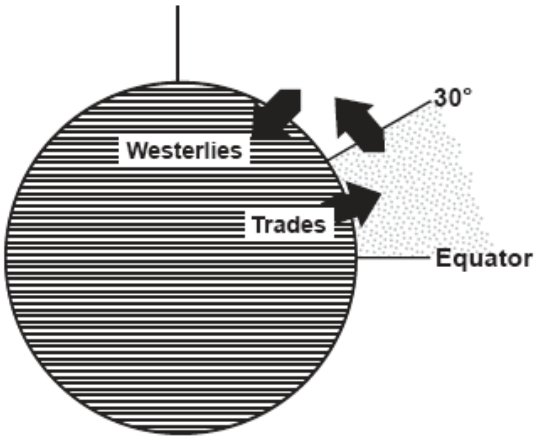

Fig. 2.8 Balance requirement for a poleward transport of angular momentum across 30° latitude.

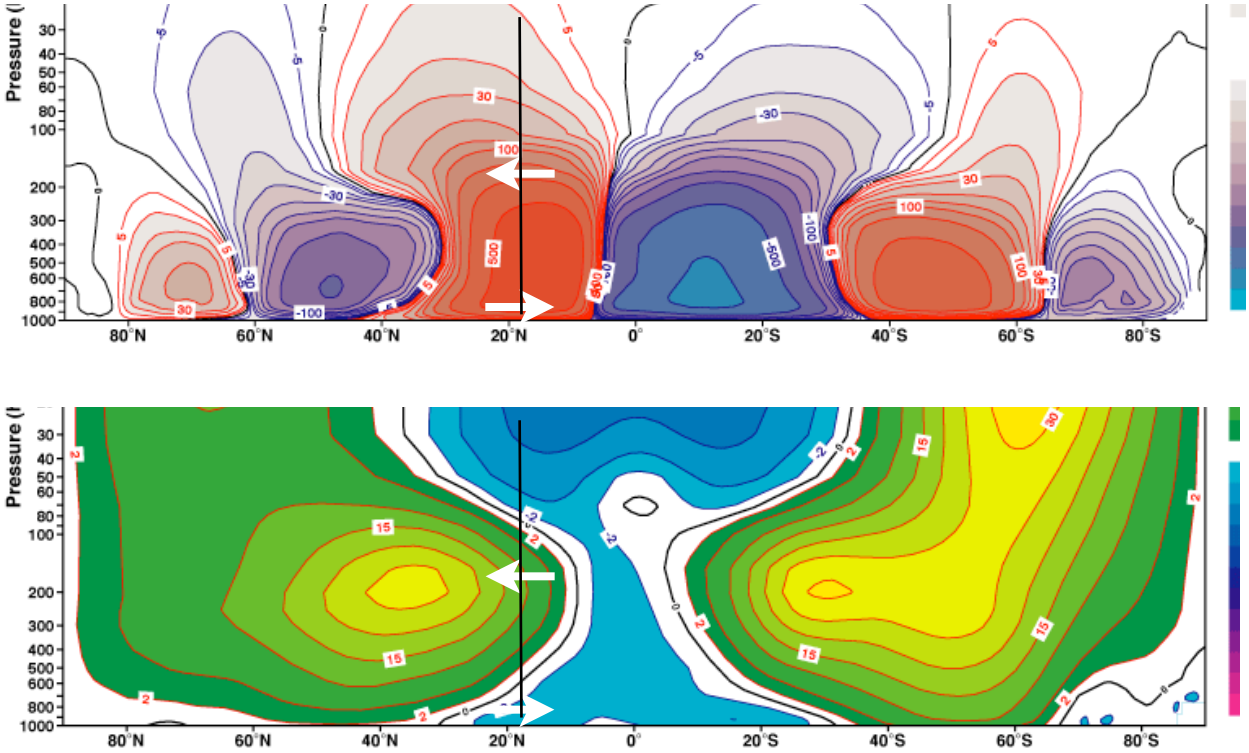

Fig. 2.9 Zonally averaged mean meridional circulations (top panel) and zonally averaged zonal wind (bottom panel) based on the ERA-40 Reanalysis. Arrows ondicate mass fluxes

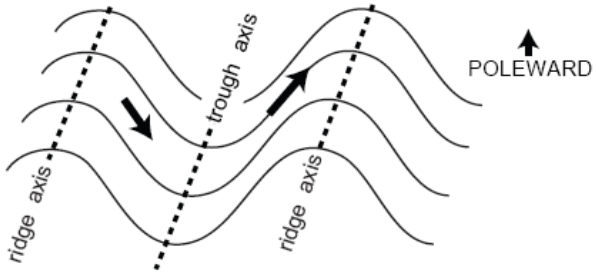

2.10 Idealized pattern of the geopotential height or streamfunction for eddies that produce a poleward transport of angular momentum.

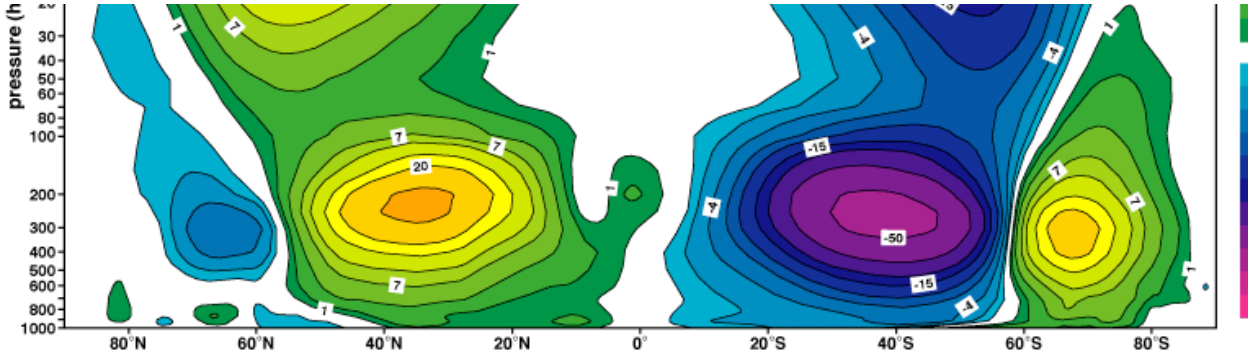

2.11 Annual mean northward transport of westerly momentum by the transient eddies. Based on the ERA-40 Reanalyses.

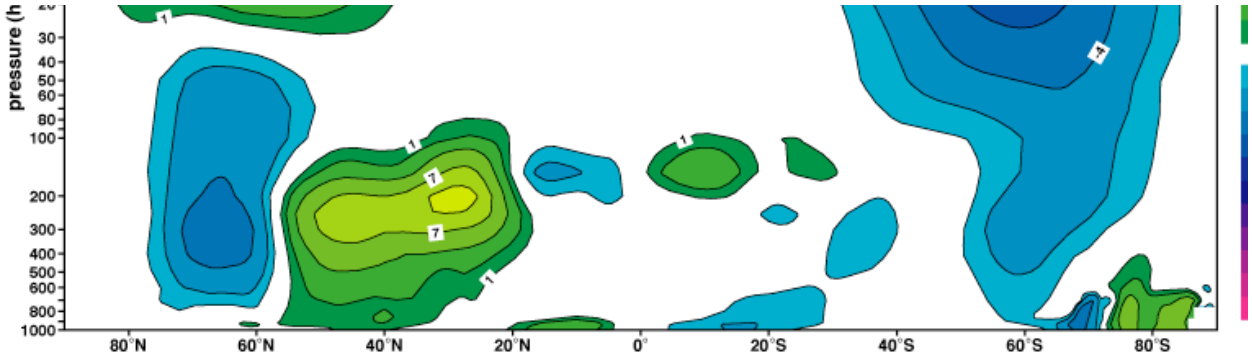

2.12 Annual mean northward transport of westerly momentum by the standing eddies or stationary waves. Based on the ERA-40 Reanalyses.

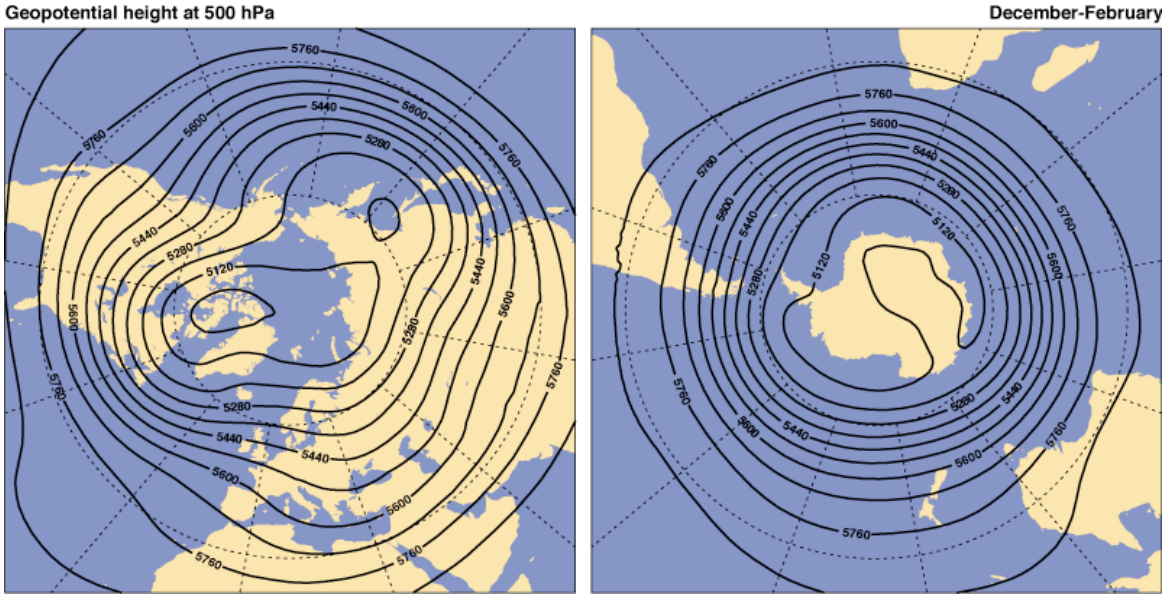

Fig. 2.13 Staionary waves in the 500 hPa DJF geopotential height field

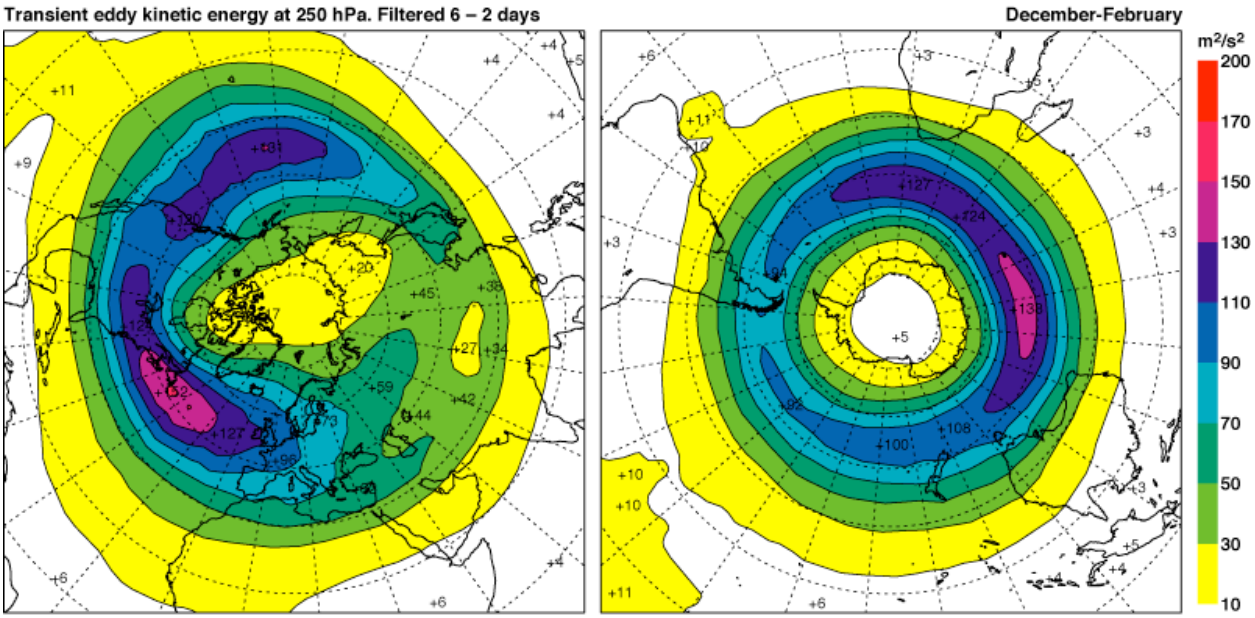

Fig. 2.14 Highpass filtered transient eddy kinetic energy at the 250-hPa level based on the ERA-40 Reanalyses.

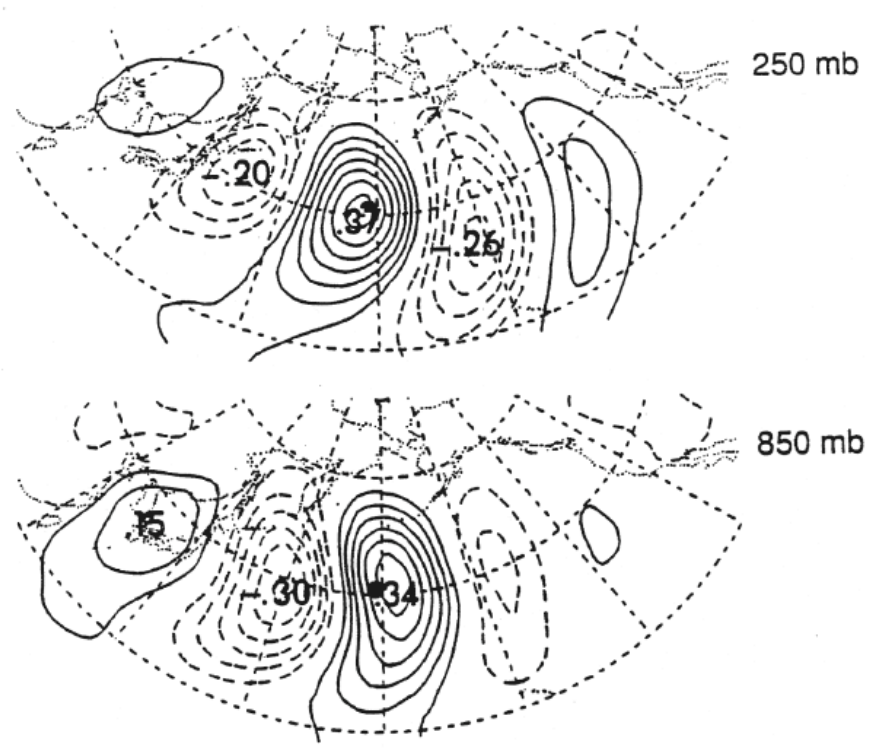

Fig. 2.15 One point correlation maps based on a highpass filtered 500 mb height time series at the gridpoint indicated by the heavy dot over the central North Pacific: DJF data for 11 winters. Upper panel 250 mb height; lower panel 850 mb height. Contour interval 0.05. Dashed contours denote negative correlations with the reference time series. After Lim (1989).

Diagrams for Chapter 2

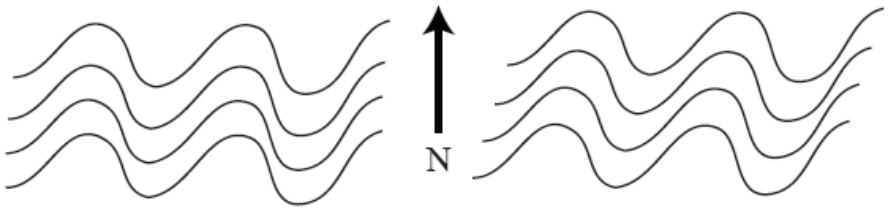

Sketch for Exercise. 2.17.

Fig. 2.16 Streamlines for the frictionally induced flow in a rotating cylinder during "spindown". The outer part of the cylinder and the parabolic free surface are not shown. After Holton (1979).

Fig. 2.18 Meridional profiles of zonal velocity of the rotating Earth and the atmosphere in absolute coordinates, and angular momentum divided by the radius of the Earth, based upon Northern Hemisphere data for the 200 mb level for DJF.

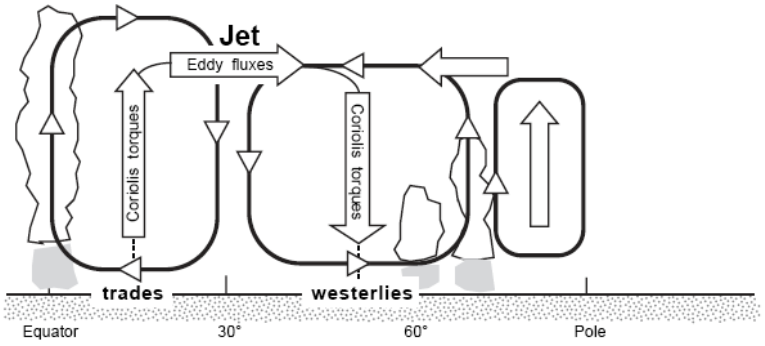

Fig. 2.17 Schematic of the transport of atmospheric angular momentum in the Earth's atmosphere. Lettering A, B, C, D to be added.

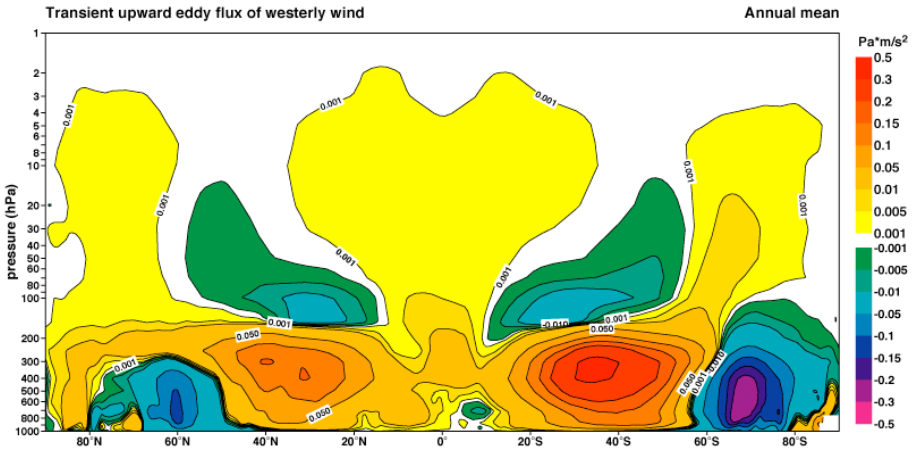

Fig. 2.18 Annual mean upward flux of westerly momentum by the transient eddies, based on the ERA-40 Reanalysis.

Diagrams for Chapter 2

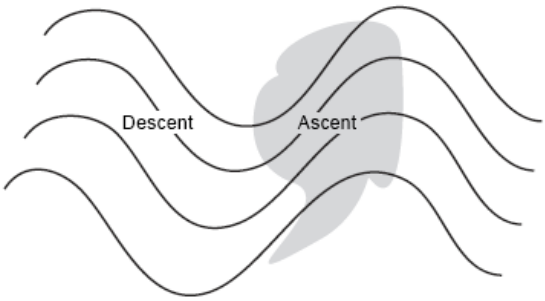

Fig. 2.19 Schematic of the structure of a typical baroclinic wave with ascent in the region of poleward flow. The northeast-to-southwest tilt of the wave axes results in an upward wddy flux of westerly momentum.

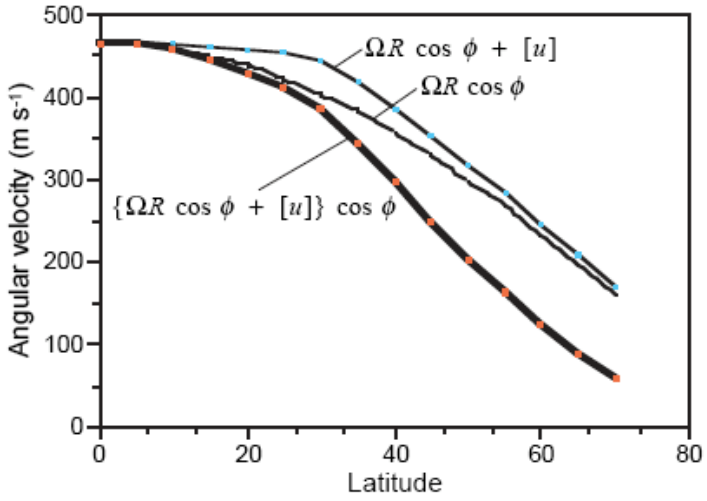

Fig. 2.20 Meridional profiles of angular velocity at the jet stream level, as indicated.

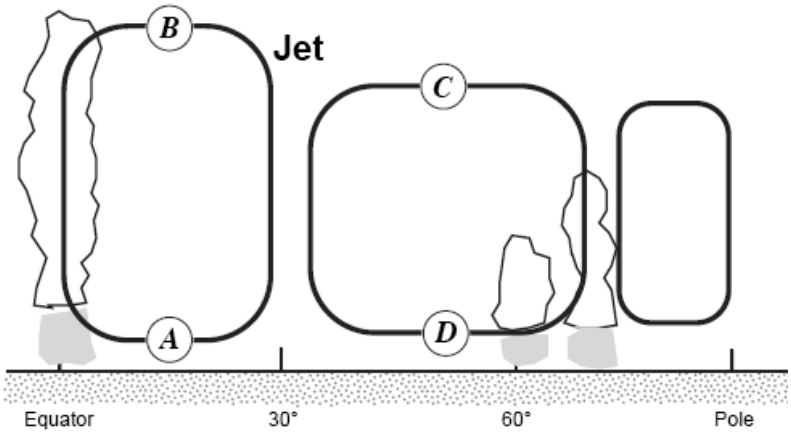

Fig. 2.21 See text for explanation.

Diagrams for Chapter 2